Harnessing Evanescent Waves by Bianisotropic Metasurfaces

*Lin Li, Kan Yao, Zuojia Wang, and Yongmin Liu**

The exponentially decaying nature of evanescent waves renders it difficult to capture, extract and engineer the wealth of energy and information that they can carry. Utilizing the out-of-plane electric dipoles and in-plane magnetic diploes produced by a bianisotropic C-aperture metasurface, in this work, it is shown that evanescent waves can be effectively molded. More specifically, it is demonstrated that the phase, polarization state or beam profile of the emission from evanescent waves can be controlled via the orientation of C-aperture nanostructures. The work opens a new avenue for metasurfaces to work in the critical near-field region to efficiently harness evanescent waves, and promises many potential applications, including on-chip free-electron light sources, tabletop particle detectors and near-field energy harvesting.

1. Introduction

In electromagnetics, evanescent waves are oscillating fields with energy spatially concentrated in the vicinity of an object. The existence of evanescent waves is general, ranging from the non-radiative emission of a point source, to total internal reflection at the interface between two media, and to optical surface waves such as surface plasmon/phonon polaritons. Arising from the spatial confinement, the amplitude of the local electric field or the local density of photonic states of an evanescent wave can be substantially enhanced. Owing to these unique properties, evanescent waves have been used in a wide range of areas, including optical trapping[1,2] and cooling,[3] biochemical sensing,[4] super-resolution microscopy,[5] subwavelength optical circuits,[6] as well as thermal energy extraction.[7]

Evanescent waves are also critically important in electron-induced emission. It is known that when the speed of a moving charged particle, such as an electron, is smaller than the phase velocity of light in the surrounding medium, the electromagnetic field produced by the charged particle is evanescent. Periodic gratings can be used to couple the near-field energy into the far field. This is the so-called Smith–Purcell emission.[8] In contrast, Cherenkov radiation, which is a direct emission to the far field, takes place when the speed of a moving particle exceeds the phase velocity of light.[9] There is a rapidly growing interest in novel light sources based on electron-induced emission, because they exhibit many special characteristics, such as high intensity and broad operating bandwidth.[10–13] Rationally designed structures, such as photonic crystals, metamaterials and plasmonic nanostructures, offer unprecedented means to tailor electron-photon interactions and hence control the electron-induced emission.[14–31] In spite of these exciting development, so far, few works have discussed the phase, polarization and beam profile control of electron-induced emission,[32] which are essential for tunable, on-chip, free-electron-driven light sources without additional bulky optical components.

Recognizing the universal characteristics of the evanescent wave associated with photons and moving charged particles, in this paper, we experimentally demonstrate an effective means to control the re-radiation of evanescent waves based on designer metasurfaces. Over the past several years, metasurfaces have shown remarkable capabilities and degrees of freedom to tailor the phase, amplitude and polarization of light.[33–48] Nevertheless, most of the reported metasurfaces focused on the manipulation of propagating light waves in free-space. It is equally important to harness evanescent waves, since they are inherently compatible with integrated photonics given their nature of subwavelength confinement. Indeed, some efforts have been devoted to manipulating surface plasmons[49–54] by designing an array of in-plane electric dipoles with proper spatial arrangements and relative phase differences. However, the aspect of converting the near field to far field beyond the electric dipole approximation has not been addressed. Bianisotropic structures,[32,55] which support both electric and magnetic resonances, could provide a useful approach in this regard as we will show in the present work.

As an important step towards harnessing evanescent waves and converting them to the far field with desired properties, here we use Smith–Purcell emission as an example and demonstrate an all-optical platform that both the spectral and angular responses of the Smith–Purcell emission can be manipulated by a C-aperture metasurface. We can control the phase of the emission from evanescent waves through engineering the electric

Dr. L. Li, Dr. Z. Wang, Prof. Y. Liu
Department of Mechanical and Industrial Engineering
Northeastern University
Boston, MA 02115, USA
E-mail: y.liu@northeastern.edu
Dr. K. Yao, Prof. Y. Liu
Department of Electrical and Computer Engineering
Northeastern University
Boston, MA 02115, USA

The ORCID identification number(s) for the author(s) of this article can be found under https://doi.org/10.1002/lpor.201900244

DOI: 10.1002/lpor.201900244

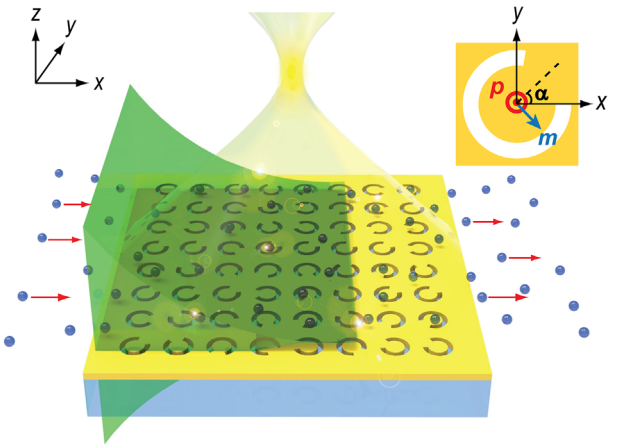

Figure 1. Schematic of harnessing evanescent waves by metasurfaces for controlling Smith–Purcell emission. Electrons (represented by blue dots) fly closely over the metasurface, which allows the associated evanescent wave (represented by the green profile) to be efficiently modulated, re-mitted and focused in free space. The yellow hyperboloid illustrates the focused Smith–Purcell emission. The phase and polarization of the emission can be controlled by the orientation arrangement of the C-apertures comprising the metasurface. The inset illustrates the produced out-of-plane electric dipole and in-plane magnetic dipole.

and magnetic dipoles via rotating the C-apertures. Then, experimentally, we use attenuated total reflection (ATR) to generate evanescent waves to mimic those produced by a swift electron beam and demonstrate the beam shaping capability of the C-aperture metasurface at optical frequencies. Moreover, the polarization states of the Smith–Purcell emission can also be controlled by adjusting the orientation of the C-apertures. Previous works on manipulating Smith–Purcell emission or converting evanescent waves into propagating waves are mainly based on the conventional diffraction or scattering process to control the amplitude of light waves. In contrast, our work presents the potential to control the phase, polarization, amplitude and beam profile of the re-emitted light from evanescent waves, which are very important for practical devices with high efficiency, compact footprint, and multiple functions. Our results not only provide a new optical platform to imitate and study intriguing electron–matter interactions, but also promise many potential applications, including compact and tunable electron-driven light sources, tabletop particle detectors and near-field energy harvesting.

Figure 1 schematically illustrates our concept of employing metasurfaces to harness evanescent waves. When electrons move closely over a C-aperture metasurface at a speed smaller than the phase velocity of light, the evanescent waves produced by the electrons can interact with the metasurface. The C-aperture exhibits strong electric and magnetic dipole resonances, resulting in an out-of-plane electric dipole $\boldsymbol{p}$ and an in-plane magnetic dipole $\boldsymbol{m}$ as shown in the inset. When excited by evanescent waves, these electric and magnetic dipoles cooperate and re-radiate energy into the far field. Different from most previous metasurface work that only utilizes electric dipoles, both electric and magnetic dipoles are important in the process studied here. By engineering the geometry and orientation angle (α) of the C-apertures, we can control the important characteristics of the emitted light, including phase, beam profile, polarization state and wavefront. In our all-optical analogue experiments, evanescent waves are generated by ATR to mimic those produced by moving electrons, while the essential mechanism of the near-field to far-field conversion is the same.

2. Results and Discussion

To date, most of the metasurfaces for phase control are based on either the resonance phase provided by an array of different resonant nanoantennas for linearly polarized light, or the geometric phase via rotating the same building block for circularly polarized light.[34] On the other hand, for resonant nanoantennas, the required fabrication precision for phase tuning is quite challenging in the optical region, and their working bandwidth is limited compared with that based on the geometric phase. To overcome these challenges, a C-aperture metasurface is proposed, by which the phase of the re-emitted light from the evanescent waves can be well controlled via rotating the C-aperture nanostructures. When an electron beam propagates above the metasurface, it produces an evanescent wave with transverse magnetic (TM) polarization.[32] The magnetic component H_y of the evanescent wave will excite the in-plane magnetic dipole $\boldsymbol{m}_1$, which is perpendicular to the symmetry axis of the C-aperture with a phase retardation φ with respect to the excitation wave. Based on the radiation pattern of a magnetic dipole,[56] we can readily deduce that the component of $\boldsymbol{m}_1$ in the x-direction will induce the cross-polarized electric field E_{y1} in the far field and $E_{y1} \propto H_y\cos(\alpha)\sin(\alpha)$. Meanwhile, the electric component E_z of the evanescent wave can excite an out-of-plane electric dipole $\boldsymbol{p}_z$ with a phase difference of γ relative to the incident magnetic component. Because of the bianisotropy of the C-aperture, $\boldsymbol{p}_z$ will excite another in-plane magnetic dipole $\boldsymbol{m}_2$, which has the same direction as $\boldsymbol{m}_1$. Similarly, $\boldsymbol{m}_2$ will induce cross-polarized electric field E_{y2} in the far field and $E_{y2} \propto E_z\sin(\alpha)$. The overall electric field E_y is therefore given by:

$$E_y = E_{y1} + E_{y2} = E_1 \cos(\alpha)\sin(\alpha)\, e^{i\varphi} + E_2 \sin(\alpha)\, e^{i(\varphi+\gamma)} \quad (1)$$

Due to the different amplitudes $E_{1,2}$ and the relative phase difference γ, the amplitude and phase of the overall electric field E_y can be varied by rotating the C-aperture. In particular, we emphasize that the phase retardation γ between $\boldsymbol{m}_1$ and $\boldsymbol{m}_2$ is essential for modulating the phase of the emission, without which the control over the phase and wavefront for beam shaping would be impossible (see more detailed analyses based on Jones matrix in the Supporting Information).

Numerical simulations have been performed by using the particle-in-cell (PIC) solver in commercial software CST Microwave Studio, in order to investigate the characteristics of the emitted light arising from the interaction between electrons and the C-aperture metasurface.[26,57] An electron bunch with energy of 1 MeV travels 20 nm above the C-aperture metasurface. The energy of the electrons corresponds to a velocity $v = 0.94c$, here c denotes the velocity of light in the vacuum. The metasurface is composed of an array of C-apertures etched through a 100 nm-thick gold film on a glass substrate. The outer and inner radius of the C-aperture are 125 nm and 35 nm, respectively, giving rise to a strong resonance at the wavelength $\lambda = 1150$ nm. The opening

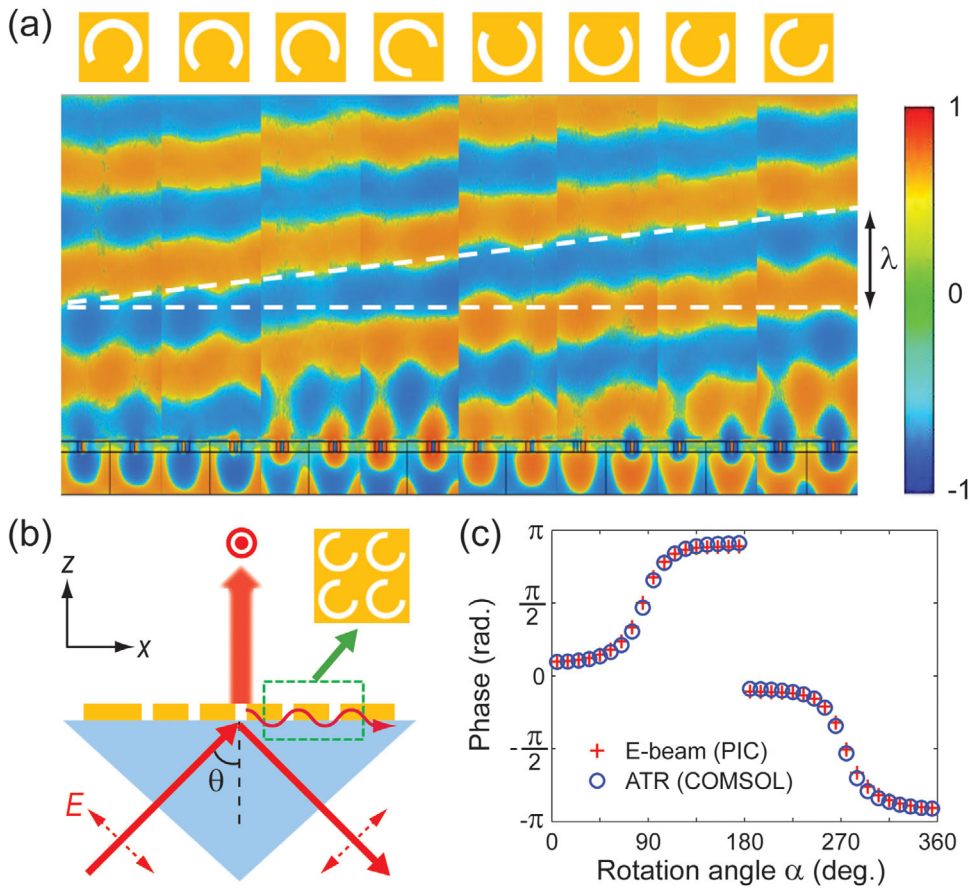

Figure 2. Numerical simulations of the phase evolution of Smith–Purcell emission modulated by C-aperture metasurfaces. a) Distribution of E_y field in the x–z plane simulated by the PIC solver. The full map consists of 8 sectors for individual C-apertures in the top inset composing the array (see the Supporting Information). b) Schematic of the all-optical analogue of Smith–Purcell emission manipulation in an ATR configuration. c) The dependence of the phase of the cross-polarized emission (E_y) on the rotation angle of C-apertures.

angle of the C-apertures is 120°, and the period in the y-direction is 450 nm. To obtain Smith–Purcell radiation along the z-axis, the period in the x-direction is chosen to be 1080 nm.[8] The simulation results are shown in **Figure 2**a (see more details in the Supporting Information). When changing the orientation of the C-apertures, one can see that the wavefront of the cross-polarized emission (E_y) has a relative optical path difference up to λ, which is equivalent to a 2π phase difference. This result manifests the feasibility of a complete control over the phase of the Smith–Purcell emission.

In order to verify the Smith–Purcell emission manipulation in an all-optical platform, we adopt the ATR configuration as shown in Figure 2b. The evanescent wave is generated by TM polarized light that is incident on a prism at an angle of incidence $\theta = 45°$. It imitates the TM evanescent wave generated by the electron beam to induce dipoles on the top surface of the metasurface, which re-radiate light to the far field ($z > 0$).[55] Full-wave simulations have been performed for the ATR configuration using the commercial software COMSOL Multiphysics. Figure 2c plots the phase of the cross-polarized emission (E_y) generated by the ATR method (blue circles) when the orientation angle of the C-apertures is varied. As discussed above, E_y is induced by the projection of the in-plane magnetic dipole along the x-axis and the sign of this component will be flipped when the C-aperture rotates across 0° and 180°, giving rise to a π-phase jump at the two angles. As a comparison, we also plot the phase diagram of the electron-induced emission simulated by PIC (red crosses). The two simulation results are in excellent agreement, unambiguously showing the validity of mimicking Smith–Purcell emission manipulation by the ATR configuration.

We have designed a metasurface with C-apertures that can simultaneously convert evanescence waves to propagating waves and focus the re-emitted light. This would open up a new paradigm for highly compact light sources. For a wave propagating along the z-axis, under the paraxial approximation, the required phase profile to focus it is quadratic, that is, $\psi(r) = -k_0 r^2/2f$, where $r = \sqrt{x^2 + y^2}$, f is the focal length and k_0 is the wave vector. The phase provided by the metasurface at (x, y) is thus $\varphi_m(x, y) = \psi(r) - nk_0 x \sin(\theta)$, where $n = 1.5$ is the refractive index of the glass substrate and $\theta = 45°$ is the angle of incidence. φ_m is implemented by varying the orientation of the C-apertures determined from the phase evolution shown in Figure 2c. The

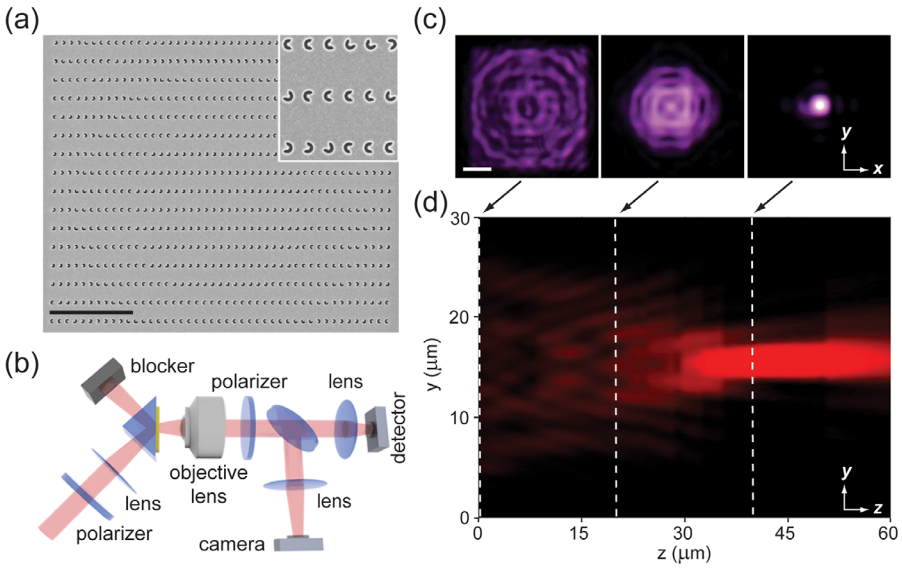

Figure 3. Experimental demonstration of phase manipulation and focusing effect by the C-aperture metasurface. a) SEM image of the sample fabricated by FIB. Scale bar: 5 μm. b) Schematic of optical measurement set-up. c) The images recorded by a CCD camera at the planes of $z = 0$, 20 and 40 μm, respectively. The intensity of light in the first two panels are multiplied by 4 for better visualization. Scale bar: 5 μm. d) The focusing image in the y–z plane.

parameters of the C-apertures are the same as those used in the numerical simulations and the working wavelength is 1150 nm.

The sample was fabricated by focused ion beam (FIB) milling through a 100 nm-thick gold film that was deposited with an e-beam evaporator on a glass substrate. The scanning electron microscope (SEM) image of the fabricated sample is shown in **Figure** 3a. Figure 3b illustrates the optical measurement set-up, in which the sample was attached to the glass prism with refractive-index matching oil. A TM-polarized laser beam was focused and incident on the prism at 45°. The emitted light manipulated by the C-aperture metasurface was collected by an objective lens (40X, NA = 0.55, Olympus) and its polarization state can be analyzed by a polarizer. By adjusting the objective along the z-axis at a step length of 1 μm, we recorded the cross-sectional images of the intensity distributions for cross-polarized light via a CCD camera in the x–y plane at different distances from the metasurface. Figure 3c presents typical recorded images in the x–y planes, located at the distances of 0, 20 and 40 μm away from the metasurface, respectively. From these images, we retrieved the intensity along the y-axis from the center of the images and reconstructed the beam profile in the y–z plane as depicted in Figure 3d. One can clearly observe the focusing effect with a predesigned focal length of $f = 40$ μm. These results confirm the capability of the C-aperture metasurface for the phase manipulation and beam shaping of the re-radiation of evanescent waves.

In the following, we will demonstrate that the C-aperture metasurface can control the polarization state of the emission as well. To fully manifest this strategy, the first task is chosen to maximize the polarization conversion ratio (PCR). For an evanescent wave polarized in the x-direction, there are two channels to produce cross-polarized emission (E_y) in the far field as we have discussed. In order to realize a high polarization conversion ratio, the C-aperture should be oriented along the y-axis, by which the in-plane magnetic dipole $\boldsymbol{m}$ can only be excited by the out-of-plane electric dipole (p_z) and oriented along the x-axis, leading to an emission only polarized along the y-axis (see more detailed discussions in the Supporting Information).

We have performed full-wave simulations in the same configuration as in Figure 2b to investigate the polarization state of the re-emitted light. The electric field distributions at the wavelength of $\lambda = 1150$ nm is shown in **Figure** 4a for two conditions. Each of them has two vertical cutting planes intersecting at the center of a C-aperture resonator to show the snapshots of E_x in the x–z plane and of E_y in the y–z plane, respectively. The emitted light is purely x-polarized ($E_y \approx 0$) when the C-apertures are oriented along the x-axis ($\alpha = 0°$, left panel), whereas when the C-apertures are oriented along the y-axis ($\alpha = 90°$, right panel), the TM evanescent wave is converted into propagating light with the orthogonal polarization state ($E_x \approx 0$). These results clearly show that efficient polarization conversion of the emission can be achieved by varying the orientation of the C-aperture resonators. To achieve highest PCR, the C-aperture should be further rotated to $\alpha \approx 100°$, so that E_x approaches to 0 (see details in the Supporting Information). In Figure 4b, we plot the simulated spectra of the normalized emission intensity of the two orthogonal polarization states, and the polarization conversion ratio defined as $\mathrm{PCR} = I_{yx}/(I_{xx} + I_{yx})$, where I_{xx} and I_{yx} are the intensities of re-emitted light polarized along the x- and y-axis, respectively. The PCR can reach almost unity around the wavelength of 1100 nm. The experimental results measured with the same optical set-up shown in Figure 3b are depicted in Figure 4c. Due to the imperfect fabrication, the intensity peak of the cross-polarization becomes broader and PCR does not reach unity (see the Supporting Information). However, the experimentally achieved PCR is still as high as 0.93, showing a very good polarization conversion with a single layer metasurface. These results demonstrate efficient polarization conversion performance over a reasonably broad bandwidth. It is worth pointing out that the broadband high PCR performance could be achieved by a metasurface with deep-subwavelength thickness (see the Supporting Information).

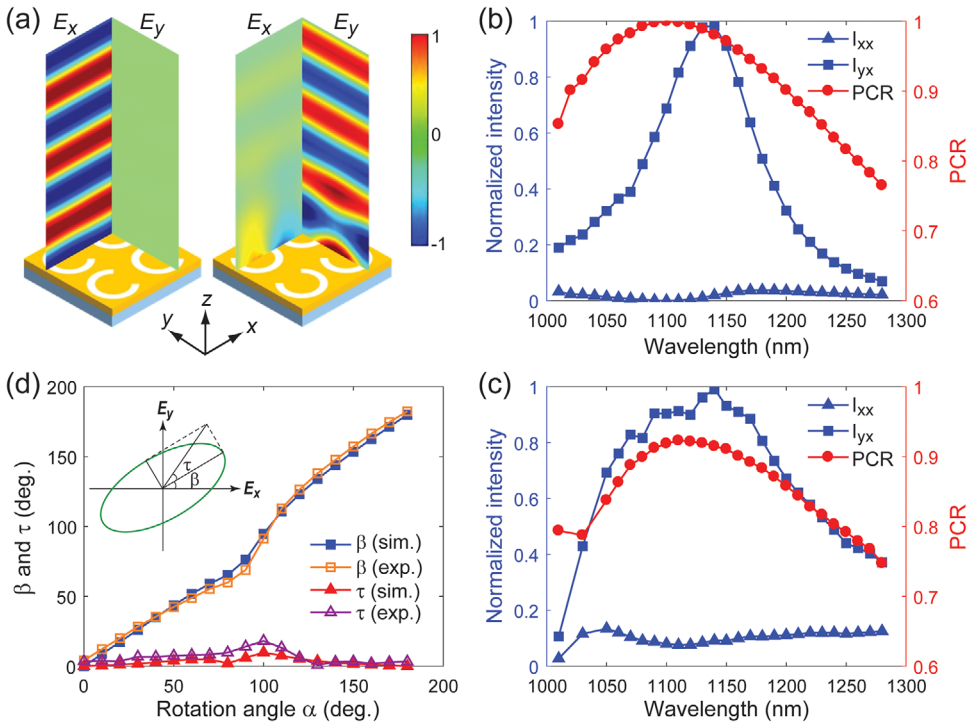

Figure 4. Demonstration of the polarization control of the emission. a) Electric fields re-emitted by the metasurface composed of the C-apertures with rotation angle $\alpha = 0°$ (left panel) and $\alpha = 90°$ (right panel). The simulated b) and experimental c) spectra of the co-polarization (I_{xx}) and cross-polarization (I_{yx}), together with the polarization conversion ratio (PCR). d) The simulated and experimental polarization states of light re-emitted by the C-aperture metasurface. The inset illustrates the general polarization ellipse.

Furthermore, the direction of the polarization can be well controlled by arranging the orientation of the C-aperture. The total electric field of the emitted light can be expressed as

$$\vec{E} = \vec{E}_x + \vec{E}_y = E_x \cos\left(kz - \omega t + \varphi_x\right)\vec{x} + E_y \sin\left(kz - \omega t + \varphi_y\right)\vec{y} \quad (2)$$

Generally, there is a phase difference of $\delta = \varphi_y - \varphi_x$, so that the emitted light is elliptically polarized as shown in the inset of Figure 4d, where β is the orientation angle and τ is the ellipticity angle.[58] Figure 4d compares the numerically simulated and experimentally extracted dependence of β and τ on the orientation of the C-aperture metasurface. The ellipticity angle τ is small in both experimental and numerical results, revealing the nearly linear polarization state of the emission from the C-aperture metasurface. The orientation angle β continuously varies with the rotation of the C-apertures. The slight difference between the rotation angle α of the C-aperture and β is caused by the direct transmission of the co-polarization (E_x) (see the Supporting Information).

In principle, the manipulation of the re-radiation of evanescent waves can be readily achieved over a broad wavelength range in the visible, infrared and even terahertz region, by properly designing the metasurface. In addition, the opening angle and the size of the C-apertures can be involved to realize the potential control of the amplitude together with the phase and polarization. Based on Babinet's principle, one can also use the complementary structure, that is, C-ring metasurface, to control evanescent waves with transverse electric (TE) polarization.[56,59–61] Finally, all-dielectric structures can support both electric and magnetic resonances with smaller optical loss than the metallic counterparts,[62,63] which are worth of investigation for the control of evanescent waves.

3. Conclusion

In conclusion, we have demonstrated a feasible scheme of manipulating the phase, beam profile and polarization of the re-radiation of evanescent waves by a bianisotropic C-aperture metasurface. The experiment can be considered as an all-optical analogue of Smith–Purcell emission. The phase of the emission is determined by the cooperation of a magnetic dipole and an electric dipole, which are induced via the in-plane magnetic field and out-of-plane electric field of a TM evanescent wave generated by the ATR configuration, respectively. The phase of the emission can be tuned by changing the orientation of the C-apertures to cover a full range of 2π. This allows us to design and realize a metasurface lens that can focus the emission at a prescribed position. In addition, the polarization of the emission can be continuously changed by rotating the orientation of the C-apertures. Because the existence of evanescent waves is universal, our approach could be applied to other systems, such as photonic waveguide modes and surface plasmon/phonon polaritons. We envision that our research findings will substantially advance integrated photonic and electro-optical devices for various applications, including on-chip free-electron light sources, optical imaging and sensing, polarization-sensitive detectors and near-field energy harvesting.

Supporting Information

Supporting Information is available from the Wiley Online Library or from the author.

Acknowledgements

The authors acknowledge the financial support from the Office of Naval Research (N00014-16-1-2409), and the National Science Foundation (ECCS-1916839). They thank Xiaokang Bai for the help on the figure preparation.

Conflict of Interest

The authors declare no conflict of interest.

Received: July 26, 2019
Revised: August 14, 2020
Published online:

[1] E. Vetsch, D. Reitz, G. Sague, R. Schmidt, S. T. Dawkins, A. Rauschenbeutel, *Phys. Rev. Lett.* **2010**, *104*, 203603.
[2] K. Okamoto, S. Kawata, *Phys. Rev. Lett.* **1999**, *83*, 4534.
[3] Y. B. Ovchinnikov, I. Manek, R. Grimm, *Phys. Rev. Lett.* **1997**, *79*, 2225.
[4] J. B. Jensen, L. H. Pedersen, P. E. Hoiby, L. B. Nielsen, T. P. Hansen, J. R. Folkenberg, J. Riishede, D. Noordegraaf, K. Nielsen, A. Carlsen, A. Bjarklev, *Opt. Lett.* **2004**, *29*, 1974.
[5] Z. W. Liu, N. Fang, T. J. Yen, X. Zhang, *Appl. Phys. Lett.* **2003**, *83*, 5184.
[6] M. L. Brongersma, V. M. Shalaev, *Science* **2010**, *328*, 440.
[7] S. Shen, A. Narayanaswamy, G. Chen, *Nano Lett.* **2009**, *9*, 2909.
[8] S. J. Smith, E. M. Purcell, *Phys. Rev.* **1953**, *92*, 1069.
[9] P. A. Cherenkov, *Dokl. Akad. Nauk SSSR* **1934**, *2*, 451.
[10] J. Urata, M. Goldstein, M. F. Kimmitt, A. Naumov, C. Platt, J. E. Walsh, *Phys. Rev. Lett.* **1998**, *80*, 516.
[11] S. E. Korbly, A. S. Kesar, J. R. Sirigiri, R. J. Temkin, *Phys. Rev. Lett.* **2005**, *94*, 054803.
[12] L. J. Wong, I. Kaminer, O. Ilic, J. D. Joannopoulos, M. Soljacic, *Nat. Photonics* **2016**, *10*, 46.
[13] G. Adamo, K. F. MacDonald, Y. H. Fu, C. M. Wang, D. P. Tsai, F. J. G. de Abajo, N. I. Zheludev, *Phys. Rev. Lett.* **2009**, *103*, 113901.
[14] S. G. Liu, P. Zhang, W. H. Liu, S. Gong, R. B. Zhong, Y. X. Zhang, M. Hu, *Phys. Rev. Lett.* **2012**, *109*, 153902.
[15] F. J. G. de Abajo, *Rev. Mod. Phys.* **2010**, *82*, 209.
[16] W. W. Li, W. H. Liu, Q. K. Jia, *AIP Adv.* **2016**, *6*, 035202.
[17] J. R. M. Saavedra, D. Castells-Graells, F. J. G. de Abajo, *Phys. Rev. B* **2016**, *94*, 035418.
[18] G. Adamo, J. Y. Ou, J. K. So, S. D. Jenkins, F. De Angelis, K. F. MacDonald, E. Di Fabrizio, J. Ruostekoski, N. I. Zheludev, *Phys. Rev. Lett.* **2012**, *109*, 217401.
[19] F. J. G. de Abajo, *ACS Nano* **2013**, *7*, 11409.
[20] T. E. Stevens, J. K. Wahlstrand, J. Kuhl, R. Merlin, *Science* **2001**, *291*, 627.
[21] C. Luo, M. Ibanescu, S. G. Johnson, J. D. Joannopoulos, *Science* **2003**, *299*, 368.
[22] V. V. Vorobev, A. V. Tyukhtin, *Phys. Rev. Lett.* **2012**, *108*, 184801.
[23] S. Xi, H. S. Chen, T. Jiang, L. X. Ran, J. T. Huangfu, B. I. Wu, J. A. Kong, M. Chen, *Phys. Rev. Lett.* **2009**, *103*, 194801.
[24] I. Kaminer, Y. T. Katan, H. Buljan, Y. C. Shen, O. Ilic, J. J. Lopez, L. J. Wong, J. D. Joannopoulos, M. Soljacic, *Nat. Commun.* **2016**, *7*, 11880.
[25] I. Kaminer, S. E. Kooi, R. Shiloh, B. Zhen, Y. Shen, J. J. López, R. Remez, S. A. Skirlo, Y. Yang, J. D. Joannopoulos, A. Arie, M. Soljačić, *Phys. Rev. X* **2017**, *7*, 011003.
[26] Z. Y. Duan, X. F. Tang, Z. L. Wang, Y. B. Zhang, X. D. Chen, M. Chen, Y. B. Gong, *Nat. Commun.* **2017**, *8*, 14901.
[27] P. Genevet, D. Wintz, A. Ambrosio, A. She, R. Blanchard, F. Capasso, *Nat. Nanotechnol.* **2015**, *10*, 804.
[28] F. Liu, L. Xiao, Y. Ye, M. X. Wang, K. Y. Cui, X. Feng, W. Zhang, Y. D. Huang, *Nat. Photonics* **2017**, *11*, 289.
[29] D. Ziemkiewicz, S. Zielinska-Raczynska, *J. Opt. Soc. Am. B* **2015**, *32*, 1637.
[30] Z. X. Su, F. Cheng, L. Li, Y. M. Liu, *ACS Photonics* **2019**, *6*, 1947.
[31] Z. X. Su, B. Xiong, Y. H. Xu, Z. Q. Cai, J. B. Yin, R. W. Peng, Y. M. Liu, *Adv. Opt. Mater.* **2019**, *7*, 1801666.
[32] Z. J. Wang, K. Yao, M. Chen, H. S. Chen, Y. M. Liu, *Phys. Rev. Lett.* **2016**, *117*, 157401.
[33] N. F. Yu, P. Genevet, M. A. Kats, F. Aieta, J. P. Tetienne, F. Capasso, Z. Gaburro, *Science* **2011**, *334*, 333.
[34] N. F. Yu, F. Capasso, *Nat. Mater.* **2014**, *13*, 139.
[35] X. J. Ni, N. K. Emani, A. V. Kildishev, A. Boltasseva, V. M. Shalaev, *Science* **2012**, *335*, 427.
[36] L. L. Huang, X. Z. Chen, H. Muhlenbernd, G. X. Li, B. F. Bai, Q. F. Tan, G. F. Jin, T. Zentgraf, S. Zhang, *Nano Lett.* **2012**, *12*, 5750.
[37] G. X. Zheng, H. Muhlenbernd, M. Kenney, G. X. Li, T. Zentgraf, S. Zhang, *Nat. Nanotechnol.* **2015**, *10*, 308.
[38] T. Li, S. M. Wang, J. X. Cao, H. Liu, S. N. Zhu, *Appl. Phys. Lett.* **2010**, *97*, 261113.
[39] L. Li, T. Li, X. M. Tang, S. M. Wang, Q. J. Wang, S. N. Zhu, *Light: Sci. Appl.* **2015**, *4*, e330.
[40] L. X. Liu, X. Zhang, M. Kenney, X. Su, N. Xu, C. Ouyang, Y. Shi, J. Han, W. Zhang, S. Zhang, *Adv. Mater.* **2014**, *26*, 5031.
[41] N. K. Grady, J. E. Heyes, D. R. Chowdhury, Y. Zeng, M. T. Reiten, A. K. Azad, A. J. Taylor, D. A. R. Dalvit, H. T. Chen, *Science* **2013**, *340*, 1304.
[42] S. M. Wang, P. C. Wu, V.-C. Su, Y.-C. Lai, C. H. Chu, J.-W. Chen, S.-H. Lu, J. Chen, B. Xu, C.-H. Kuan, T. Li, S. Zhu, D. P. Tsai, *Nat. Commun.* **2017**, *8*, 187.
[43] A. Arbabi, Y. Horie, M. Bagheri, A. Faraon, *Nat. Nanotechnol.* **2015**, *10*, 937.
[44] A. Arbabi, E. Arbabi, Y. Horie, S. M. Kamali, A. Faraon, *Nat. Photonics* **2017**, *11*, 415.
[45] D. M. Lin, P. Y. Fan, E. Hasman, M. L. Brongersma, *Science* **2014**, *345*, 298.
[46] A. E. Minovich, A. E. Miroshnichenko, A. Y. Bykov, T. V. Murzina, D. N. Neshev, Y. S. Kivshar, *Laser Photonics Rev.* **2015**, *9*, 195.
[47] L. Wang, S. Kruk, H. Z. Tang, T. Li, I. Kravchenko, D. N. Neshev, Y. S. Kivshar, *Optica* **2016**, *3*, 1504.
[48] Y. C. Lai, T. C. Kuang, B. H. Cheng, Y. C. Lan, D. P. Tsai, *Sci. Rep.* **2017**, *7*, 11096.
[49] D. Wintz, P. Genevet, A. Ambrosio, A. Woolf, F. Capasso, *Nano Lett.* **2015**, *15*, 3585.
[50] J. Lin, J. P. B. Mueller, Q. Wang, G. H. Yuan, N. Antoniou, X. C. Yuan, F. Capasso, *Science* **2013**, *340*, 331.
[51] W. B. Chen, D. C. Abeysinghe, R. L. Nelson, Q. W. Zhan, *Nano Lett.* **2010**, *10*, 2075.
[52] L. L. Huang, X. Z. Chen, B. F. Bai, Q. F. Tan, G. F. Jin, T. Zentgraf, S. Zhang, *Light: Sci. Appl.* **2013**, *2*, e70.
[53] H. Y. Shi, J. X. Li, A. X. Zhang, Y. S. Jiang, J. F. Wang, Z. Xu, S. Xia, *IEEE Antennas and Wirel. Propag. Lett.* **2015**, *14*, 104.
[54] Y. Ling, L. Huang, W. Hong, T. Liu, L. Jing, W. Liu, Z. Wang, *Opt. Express* **2017**, *25*, 29812.
[55] F. Falcone, T. Lopetegi, M. A. G. Laso, J. D. Baena, J. Bonache, M. Beruete, R. Marques, F. Martin, M. Sorolla, *Phys. Rev. Lett.* **2004**, *93*, 197401.
[56] J. D. Jackson, *Classical Electrodynamics*, 3rd ed., Wiley, New York **1999**.
[57] J. K. So, J. H. Won, M. A. Sattorov, S. H. Bak, K. H. Jang, G. S. Park, D. S. Kim, F. J. Garcia-Vidal, *Appl. Phys. Lett.* **2010**, *97*, 151107.

[58] M. Born, E. Wolf, *Principles of Optics : Electromagnetic Theory of Propagation, Interference and Diffraction of Light*, 7th expanded ed., Cambridge University Press, Cambridge **1999**.
[59] T. Zentgraf, T. P. Meyrath, A. Seidel, S. Kaiser, H. Giessen, C. Rockstuhl, F. Lederer, *Phys. Rev. B* **2007**, *76*.
[60] X. J. Ni, S. Ishii, A. V. Kildishev, V. M. Shalaev, *Light: Sci. Appl.* **2013**, *2*, e72.
[61] J. Kim, Y.-G. Roh, S. Cheon, J.-H. Choe, J. Lee, J. Lee, H. Jeong, U. J. Kim, Y. Park, I. Y. Song, Q. H. Park, S. W. Hwang, K. Kim, C.-W. Lee, *Nano Lett.* **2014**, *14*, 3072.
[62] S. M. Kamali, E. Arbabi, A. Arbabi, A. Faraon, *Nanophotonics* **2018**, *7*, 1041.
[63] S. Jahani, Z. Jacob, *Nat. Nanotechnol.* **2016**, *11*, 23.